Differentiation (2003) 71:542–548

ORIGINAL ARTICLE

Teresa Pellegrino · Wolfgang J. Parak
Rosanne Boudreau · Mark A. Le Gros
Daniele Gerion · A. Paul Alivisatos
Carolyn A. Larabell

Quantum dot-based cell motility assay

Accepted October 30, 2003

Abstract Motility and migration are measurable characteristics of cells that are classically associated with the invasive potential of cancer cells, but *in vitro* assays of invasiveness have been less than perfect. We previously developed an assay to monitor cell motility and migration using water-soluble CdSe/ZnS nanocrystals; cells engulf the fluorescent nanocrystals as they crawl across them and leave behind a fluorescent-free trail. We show here that semiconductor nanocrystals can also be used as a sensitive two-dimensional *in vitro* invasion assay. We used this assay to compare the behavior of seven different adherent human cell lines, including breast epithelial MCF 10A, breast tumor MDA-MB-231, MDA-MB-435S, MCF 7, colon tumor SW480, lung tumor NCI H1299, and bone tumor Saos-2, and observed two distinct behaviors of cancer cells that can be used to further categorize these cells. Some cancer cell lines demonstrate fibroblastic behaviors and leave long fluorescent-free trails as they migrate across the dish, whereas other cancer cells leave clear zones of varying sizes around their periphery. This assay uses fluorescence detection, requires no processing, and can be used in live cell studies. These features contribute to the increased sensitivity of this assay and make it a powerful new tool for discriminating between non-invasive and invasive cancer cell lines.

Key words invasion assay · motility · metastatic potential · phagokinetic track · fluorescent colloidal semiconductor quantum dots

Teresa Pellegrino · Wolfgang J. Parak · Daniele Gerion · A. Paul Alivisatos
Department of Chemistry
University of California, Berkeley
Berkeley, CA 94720, USA

Rosanne Boudreau · Mark A. Le Gros · A. Paul Alivisatos · Carolyn A. Larabell
Life Sciences Division
Lawrence Berkeley National Laboratory
Berkeley, CA 94720, USA

Carolyn A. Larabell (✉)
Department of Anatomy
University of California, San Francisco
San Francisco, CA 94143, USA
Fax: (415) 476-4845
E-mail: larabel@itsa.ucsf.edu

Introduction

The ability of tumor cells to invade surrounding tissue and to metastasize to different sites in the body is known to be related to the motility of the cells. Various assays have been used to study cell invasiveness *in vitro*. The goal is to correlate *in vitro* invasive assays with the *in vivo* metastatic potential of the tumor cells. The most widely used assay is the Boyden chamber invasion assay (Hynda et al., 1986; Kramer et al., 1986; Terranova et al., 1986; Albini et al., 1987), where the ability of the cell to pass through a matrix of basement membrane (BM) is evaluated. Although it is a reasonable model to study cell invasiveness, it fails in some cases to describe the complex *in vivo* situation: some malignant cancer cells that are invasive *in vivo* are not able to cross the BM matrix (Noel et al., 1991; de Both et al., 1999). Here we present an assay that distinguishes between these two types of cell lines and that can provide a rapid, robust, and quantitative *in vitro* measure of metastatic potential.

To probe the metastatic potential of different cancer cell lines, we have developed a two-dimensional *in vitro* invasion assay using water-soluble CdSe/ZnS nanocrystals. Colloidal CdSe/ZnS semiconductor nanocrystals, also called quantum dots, are robust inorganic fluorophores (Murray et al., 1993; Alivisatos, 1996; Hines and Guyotsionnest, 1996; Dabbousi et al., 1997): when

U.S. Copyright Clearance Center Code Statement: 0301–4681/2003/7109–542 $ 15.00/0

excited with UV light, fluorescence in the visible range is emitted and their emission color is tunable by changing the size of the particle. A silica shell on the surface of the CdSe/ZnS nanocrystals makes these particles biocompatible and stable under physiological conditions (Gerion et al., 2001; Parak et al., 2002). These fluorophores are extremely robust photochemically, enabling studies of fluorescence from dots in cells on long time scales as compared to cell division (Bruchez et al., 1998; Chan and Nie, 1998; Akerman et al., 2002; Benoit et al., 2002; Chen and Rosenzweig, 2002; Rosenthal et al., 2002; Jaiswal et al., 2003; Wu et al., 2003).

It has already been shown that cells are able to engulf silanized CdSe/ZnS in a nonspecific way (Parak et al., 2002). When cancer cells are seeded on top of a homogenous layer of nanocrystals and are incubated at 37°C for 24 hr, they engulf the nanocrystals as they move and leave behind a phagokinetic track free of nanocrystals that is no longer fluorescent (Albrecht-Buehler, 1998). The area of the phagokinetic track with respect to the area of the cell can be compared between different cell lines. To assess the viability of using quantum dot-based phagokinetic tracks as indicators of metastatic potential, we compare the behavior of seven different adherent human cell lines with known behaviors from both *in vivo* secondary tumor formation studies and *in vitro* Boyden chamber invasion assays. The cell lines studied include: MCF 10A, a non-tumorigenic cell line with epithelial morphology; MDA-MB-231, a cell line derived from a mammary pleural effusion that is tumorigenic in nude mice, forming poorly differentiated adenocarcinoma; MDA-MB-435S, a cell line derived from the pleural effusion of a female with metastatic ductal carcinoma of the breast; SW480, a colorectal adenocarcinoma cell line; NCI H1299, a large carcinoma lung cell line; and Saos-2, an osteosarcoma cell line with epithelial morphology that is non-tumorigenic in immunosuppressed mice. The size and shape of the trails from each cell line were correlated with the established potential invasiveness of those cells. We show that the Quantum Dot Phagokinetic Track assay rapidly and simply discriminates between non-invasive and invasive cancer cell lines, with greater sensitivity than the Boyden chamber invasion assay, and provides a new tool for quantifying tumor cell invasiveness.

Methods

Cell cultures

MCF 10A, MCF 7, MDA-MB-231, MDA-MB-435S, SW480, NCI H1299, and Saos-2 cells were obtained from American Type Culture Collection (ATCC).

Cells were grown in the appropriate media as follows: MDA-MB-231 and SW480 cells in Leibovitz's L-15 (ATCC) supplemented with 10% fetal bovine serum (GIBCO); MDA-MB-435S cells in Leibovitz's L-15 supplemented with 0.01 mg/ml insulin and 10% fetal bovine serum; NCI H1299 cells in RPMI 1640 (ATCC) plus 5% fetal bovine serum; Saos-2 cells in McCoy's 5a (ATCC) plus 15% fetal bovine serum; MCF 7 cells in EMEM (ATCC) plus 0.01 mg/ml insulin and 10% fetal bovine serum; and MCF 10A cells in phenol red-free MEGM (mammary epithelial growth medium, serum-free) from Clonetics plus 100 ng/ml cholera toxin (Calbiochem). All cell lines were maintained as monolayer cultures, fed every 2–3 days, and passaged at 80% confluence. Passaging of all cell lines except MCF 10A was carried out using 0.25% (w/v) trypsin, 1 mM EDTA-4Na (GIBCO); MCF 10A cells were first rinsed with 3 ml of cell dissociation solution (Sigma, St. Louis, MO) and then incubated in 200 µl of fresh cell dissociation solution and 800 µl 0.05% trypsin, 0.53 mM EDTA-4Na for 15 min.The flask was gently tapped every 5 min to dislodge the cells, and the trypsin was neutralized by adding MEGM containing 20% fetal bovine serum.

Preparation of the fluorescent CdSe/ZnS nanocrystal layer and cell seeding

Assays were conducted in 4-well chambered cover glass slides (LabTEK II) coated with a thin layer of nanocrystals. Chambers were first coated with a thin layer of collagen (Cohesion, Vitrogen) by adding 400 µl of a type 1 collagen solution (0.08 mg/ml) to each well and incubating for 1 hr at 37°C. The residual collagen solution was then aspirated and a drop of water-soluble fluorescent semiconductor nanocrystals (ca. 0.2 µM) was applied to the wet collagen layer. We used red fluorescent silanized CdSe/ZnS nanocrystals of about 15 nm total outer diameter emitting at 620 nm.The chamber was left to dry under a UV lamp in a sterile hood to guarantee a sterile layer. Cells were added to the nanocrystal layer in their respective medium supplemented with 50 units/ml penicillin and 50 µg/ml streptomycin (GIBCO). To avoid the overlap of phagokinetic tracks, we used a low cell density (1000 cells/cm^2). The samples were incubated at 37°C for 24 hr.

Microscopy

Images were taken with a Bio-Rad MRC-1024 laser scanning confocal imaging system equipped with a Nikon Diaphot and a Fluor 20 ×, 0.75 NA lens. The presence of phagokinetic tracks on the fluorescence layer was detected with a krypton-argon laser while cells were imaged using a transmitted light detector. After incubation of cells at 37°C for 24 hr, images were taken using an excitation wavelength of 488 nm and long pass emission filter at 585 nm with a laser power of 10%.

Invasion assay

Invasiveness was tested for the following human cell lines: MDA-MB-231, MDA-MB-435S, MCF 7, MCF 10A, and SW480. The Boyden chamber *in vitro* invasion assay was performed using BD BioCoat Matrigel invasion chambers. Inserts contained an 8 µm pore size PET membrane coated with a layer of growth factor-reduced BD Matrigel basement membrane matrix. For each cell line, 300 µl of regular growth media free of chemoattractant was placed in the 1.5 cm diameter well below the chamber, and 10^5 cells suspended in 200 µl of regular growth media were seeded in the upper compartment of each insert. After 20 hr of incubation at 37°C, cells on the inner surface of the chamber were removed with a cotton swab, while cells that passed through the matrix were fixed in a 5% glutaraldehyde solution, stained with a 0.5% toluidine blue stain solution, and counted under an optical microscope. Cell

counts were averages from five fields of view per chamber, three chambers per cell line.

Results

As described previously (Parak et al., 2002), cells cultured on collagen coated with a thin layer of semiconductor nanocrystals adhere and spread on the substrate after the first 3 hr. After 24 hr, motile cells engulf enough nanocrystals to leave behind large clearings in the nanocrystal layer. To evaluate the individual behavior of cells seeded on the layer, here we considered only trails of single living cells 24 hr after plating.

Behavior of metastatic and *in vitro* invasive versus metastatic and *in vitro* non-invasive cells cultured on a nanocrystal layer

We examined the behavior of six human metastatic cell lines that can be distinguished by their ability to penetrate the Matrigel layer in a Boyden chamber invasion assay (to avoid confusion between differentiated, un-differentiated, and de-differentiated cells). By *in vitro* non-invasive, we mean cells that failed to pass through the basement membrane layer in a Boyden chamber, and by *in vitro* invasive, we mean cells that were able to penetrate the Matrigel substrate. The human mammary gland adenocarcinoma cell line MDA-MB-231 and the human mammary ductal carcinoma cell line MDA-MB-435S are both examples of metastatic and highly invasive (Nawrocki et al., 2001) cell lines that leave a large non-fluorescing area free of nanocrystals on the red nanocrystal layer (Fig. 1A,1B). As shown in Fig. 1Aa and 1Ba from the transmitted light imaging, the cell size is much smaller than the dark cell trail shown in Fig. 1Ac and 1Bc. Images in Fig. 1Ab and 1Bb are the superposition of the confocal and transmitted light images, showing the co-localization of the cell with respect to its corresponding phagokinetic track. In contrast, Figure 2A demonstrates the behavior of a metastatic human mammary adenocarcinoma cell line, MCF 7, which failed to pass through the Matrigel in the Boyden chamber invasion assay (Noel et al., 1991; Ree et al., 1998; Sliva et al., 2000). From the transmitted light and the confocal images (Fig. 2Aa,2Ac), it is evident that these cells are able to remove nanocrystals from the layer but the area free of nanocrystals is smaller than the cell area.

All cell lines that are known to be metastatic *in vivo*, but *in vitro* do not pass the Matrigel membrane, show a common feature in their phagokinetic tracks. Namely, substantial numbers of quantum dots on the periphery of the cells are ingested, leaving small fluorescent-free

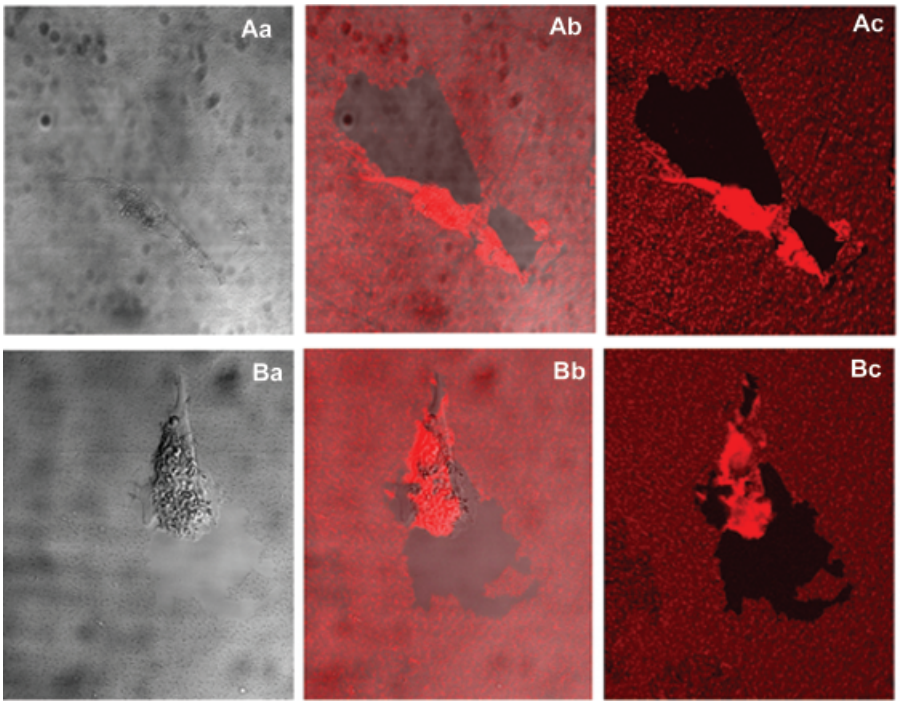

Fig. 1 Phagokinetic tracks of the highly metastatic human mammary gland adenocarcinoma cell line MDA-MB-231 (**A**) and the human mammary ductal carcinoma cell line MDA-MB-435S (**B**) grown on a collagen substrate that had been coated with a layer of silanized, water-soluble fluorescence semiconductor nanocrystals. Images were collected with a confocal microscope using a fluorescence detector to record the nanocrystal trails (Ac, Bc) and a transmitted light detector to visualize the cells (Aa, Ba); the merged pictures (Ab, Bb) co-localize the cells and the layer. After 24 hr, sizable regions free of nanocrystals, larger than the cells themselves, are detected.

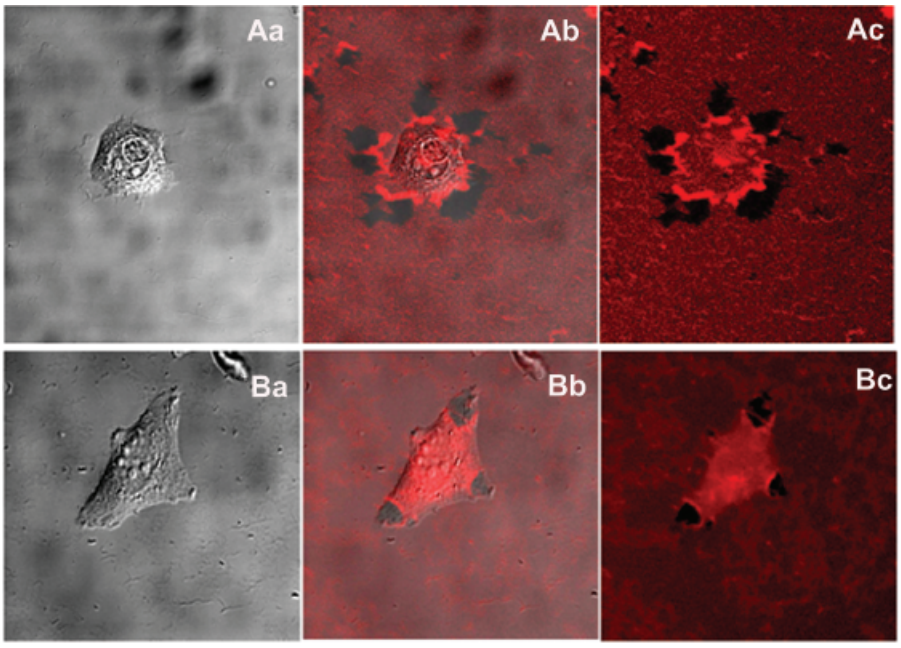

Fig. 2 Migratory paths of metastatic human mammary gland adenocarcinoma cell line MCF 7 (**A**) and human malignant colorectal adenocarcinoma cell line SW480 (**B**) on a nanocrystal layer. Transmitted light micrographs of MCF 7 and SW480 cells are shown in (Aa) and (Ba), and the fluorescence confocal pictures of the layer are shown in (Ac) and (Bc); the merged images show the cells and the layer of nanocrystals (Ab, Bb). After 24 hr, MCF 7 and SW480 cells leave a small area free of nanocrystals surrounding the cell.

zones around each cell; however, there is no detectable displacement of the cell itself. To see this point, consider the trails made by other human metastatic and *in vitro* invasive cell lines from different tissues (Li et al., 1996; Lakka et al., 2001), such as the osteosarcoma bone cell line, Saos-2 (Fig. 3A), and the large carcinoma lung cell line, NCI H1299 (Fig. 3B). These malignant cells demonstrate (Fig. 3Ac,3Bc) that increased invasiveness

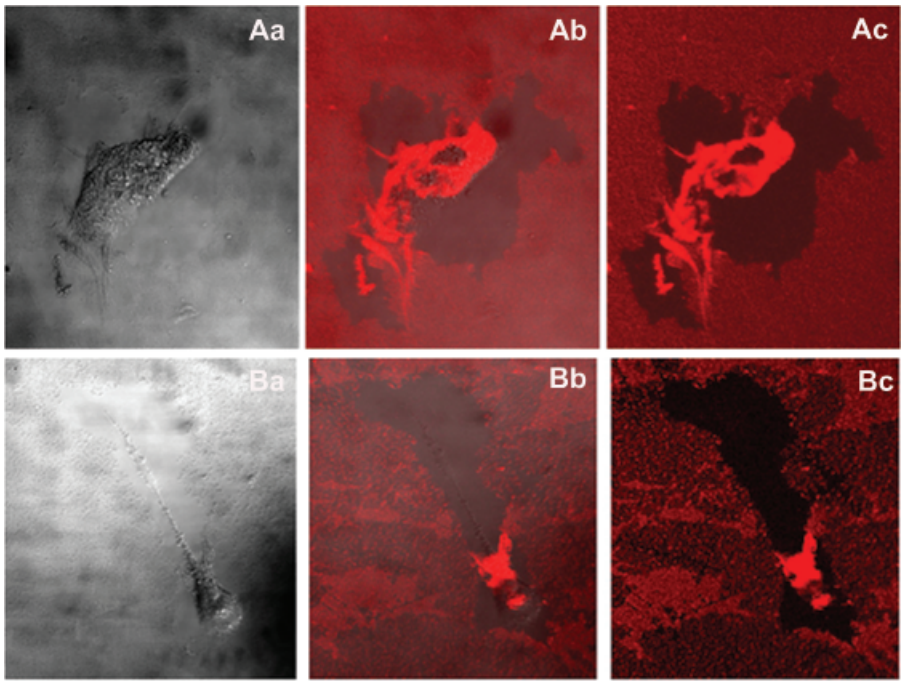

Fig. 3 Phagokinetic tracks of the osteosarcoma bone cell line Saos-2 (**A**) and the large carcinoma lung cell line NCI H1299 (**B**). Transmitted light micrographs (Aa, Ba) show the Saos-2 and NCI H1299 cells' morphology on the layer; confocal images of the layer (Ac, Bc) show the trails left by these cells; the merged pictures (Ab, Bb) show the cells and the layer of nanocrystals. After 24 hr, these cell lines leave a large dark area free of nanocrystals, considerably larger than the cell.

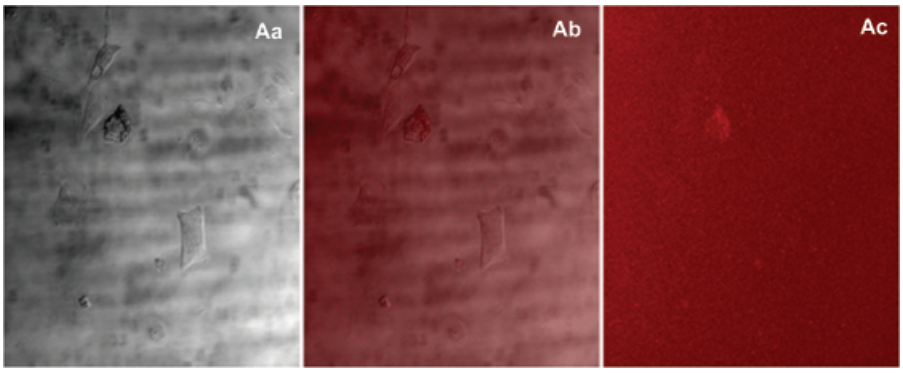

Fig. 4 Behavior of a non-tumorigenic epithelial breast cell, MCF 10A, grown on a layer of nanocrystals. The transmitted light image visualizes the cells (**A**), the fluorescence confocal image shows the nanocrystal layer (**C**), and the merged image shows the cells and the layer (**B**). After the same incubation time, 24 hr, the non-tumorigenic MCF 10A cell lines leave no detectable tracks on the layer.

corresponds with the ability to leave large areas free of nanocrystals in comparison to cell size (Fig. 3Aa,3Ba), and the center of mass of the cell has moved many diameters over a 24 hr period. In contrast, the human malignant but non-invasive (de Both et al., 1999) colorectal adenocarcinoma cell line SW480 is able to spread on the nanocrystal layer and remove nanoparticles in small regions at the edge of the cell. This cell line, like the breast MCF 7 cell line, has a center of mass that does not move and leaves a recognizable pattern free of nanocrystals that is smaller than the area of the cell. As a control, we have also compared the behavior of a non-tumorigenic epithelial breast cell line, MCF 10A. After the same incubation time, as is shown in Figure 4A, these cells are attached to the collagen layer but do not leave a trail free of nanocrystals.

Statistics on motility for the seven cell lines investigated

We collected a number of images for each cell line to statistically compare single events. In Fig. 5A and 5B, we report the plot of the ratio (trail area)/(cell area) corresponding to that trail. For each population, we estimated an average value for the most probable size of the trail per cell line. This statistic shows that MCF 7 and SW480 cells, both metastatic but *in vitro* non-invasive cell lines, have an average value of 0.9 ± 0.7 (SD, $n = 239$) and 0.5 ± 0.5 (SD, $n = 95$), respectively. We made similar measurements of a number of cell lines that are both metastatic and *in vitro* invasive, which generated ratios greater than 1.0. For example, mammary MDA-MB-435S and MDA-MB-231 cell lines yielded average ratios of 1.9 ± 1.3 (SD, $n = 262$) and 6.0 ± 3.0 (SD, $n = 183$), respectively, lung NCI H1299 (data not shown) had an average ratio of 3.8 ± 1.7 (SD, $n = 169$), and the malignant bone and *in vitro* invasive (data not shown) cell line Saos-2 had an average ratio of 3.2 ± 1.7 (SD, $n = 211$). Together, these results suggest that, under the conditions of our assay, invasive and metastatic cell lines demonstrate an average ratio of the area free of nanocrystals per cell area examined that is greater than 1, whereas metastatic but *in vitro* non-invasive cells have an average ratio less than 1.

Evaluation of invasion assay statistics

In Fig. 6A, we report the Boyden invasion assay results for five of these cell lines: MDA-MB-231, MDA-MB-435S, MCF 7, MCF 10A, and SW480. The histograms show the number of cells that cross the basement membrane for each cell line. When we performed the invasion assay without chemoattractant, we observed that the malignant cancer cell lines MDA-MB-231 and MDA-MB-435S are both highly invasive, whereas the number of cells passing through the BM was negligible for the metastatic MCF 7 and SW480 cell lines. Similarly, only a small number of cells crossed the BM when the non-tumorigenic epithelial breast cell line MCF 10A was tested for invasion in the Boyden chamber assay. These observations with respect to the Boyden chamber assay are in accord with well-known literature observations (Noel et al., 1991; Ree et al., 1998; de Both et al., 1999; Moon et al., 2000; Sliva et al., 2000; Nawrocki et al., 2001; Silvestri et al., 2002), and were performed only to show that the results on the phagokinetic tracks did not reflect random variations in the specific cell lines used.

Discussion

In principle, it is desirable to create an *in vitro* experiment that emulates just enough characteristics of a living system so as to provide a suitable model for studies of invasion and metastasis. However, it is just as important to have a simple, robust, and quantitative method that can offer a proxy for metastatic potential and that can be employed widely and used to compare

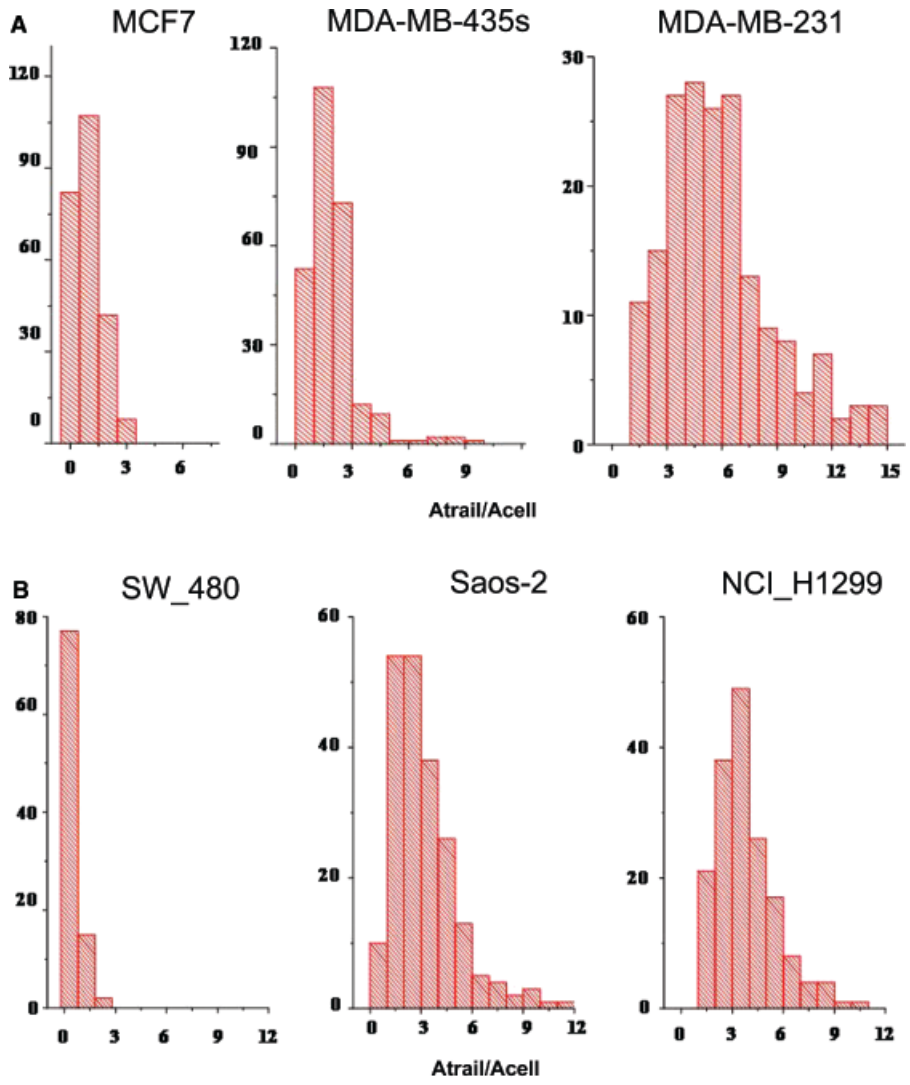

Fig. 5 (**A**) Statistics on motility of human cancer breast cell lines MDA-MB-231, MDA-MB-435S, and MCF 7. The plots show the ratio (trail area)/(cell area) versus the frequency of events. The average values for the most probable size of the trail per cell line estimated are: MDA-MB-231, 6 ± 3 (SD) on 182 pictures; MDA-MB-435S, 1.9 ± 1.3 (SD) on 262 pictures; and MCF, 70.9 ± 0.7 on 239 pictures. (**B**) Statistics on motility of human cancer cell lines SW480, NCI H1299, and Saos-2. The plots show the ratio (trail area)/(cell area) versus the frequency of events. The average values for the most probable size of the trail per cell line estimated are: SW480, 0.5 ± 0.5 (SD) on 95 pictures; NCI H1299, 3.8 ± 1.7 (SD) on 169 pictures; and Saos-2, 3.2 ± 1.7 (SD) on 211 pictures.

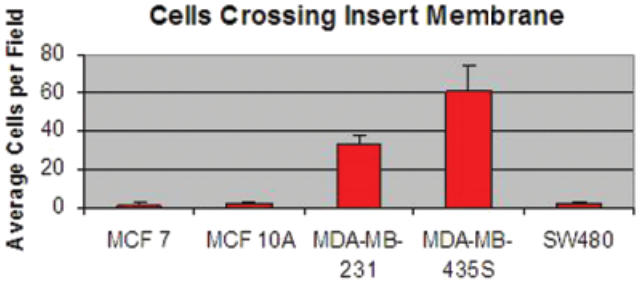

Fig. 6 *In vitro* invasion assay of MDA-MB-231, MDA-MB-435S, MCF 7, MCF 10A, and SW480. A plot showing the mean number of invasive cells for a 20 × field of view. Counts were performed on three inserts per cell line and five fields of view per insert. The error bars represent the standard deviation of the mean number of invasive cells per field of view for all fields counted per cell line.

different cell lines. To be sure, motion over a two-dimensional quantum dot layer is a less realistic simulation of the process of invasion than the invasion assay; however, the present method produces quantitative results proportional to metastatic potential for all cell lines, even ones for which the Boyden chamber invasion assay, which must be missing key features of the complex living system, produces non-physiological results. Further, the imaging of tracks can be carried out on live cells, decreasing loss of cells during processing, and can be readily automated and put under computer control so that the quantum dot phagokinetic tracking method can be implemented in a wide range of laboratories, and potentially even in clinical environments.

Acknowledgments T.P. was partially supported by Universita' degli Stuudi di Bari (Bari, Italy). W.J.P. was supported by the German Research Foundation (DFG). This work was supported by NIH grant no. R01 GM63948-01 and by the United States Department of Energy, Office of Biological and Energy Research under contract no. DE-AC03-76SF00098.

References

Akerman, M.E., Chan, W.C.W., Laakkonen, P., Bhatia, S.N. and Ruoslahti, E. (2002) Nanocrystal targeting *in vivo*. Proc Natl Acad Sci USA 99:12617–12621.

Albini, A., Iwamoto, Y., Kleinman, H.K., Martin, G.R., Aaronson, S.A., Kozlowski, J.M. and McEwan, R.N. (1987) A rapid *in vitro* assay for quantitating the invasive potential of tumor cells. Cancer Res 47:3239–3245.

Albrecht-Buehler, G. (1998) Phagokinetic track assay of cell locomotion in tissue culture. In: Spector, D.L., Goldman, R.D. and Leinwand, L.A. (eds.) Cells: a laboratory manual, Volume 2, Light microscopy and cell structure. Cold Spring Harbor Laboratory Press, Plainview, NY, pp. 77.1–77.10.

Alivisatos, A.P. (1996) Semiconductor clusters, nanocrystals, and quantum dots. Science 271:933–937.

Bruchez, M., Jr., Moronne, M., Gin, P., Weiss, S. and Alivisatos, A.P. (1998) Semiconductor nanocrystals as fluorescent biological labels. Science 281:2013–2016.

Chan, W.C.W. and Nie, S. (1998) Quantum dot bioconjugates for ultrasensitive nonisotopic detection. Science 281:2016–2018.

Chen, Y. and Rosenzweig, Z. (2002) Luminescent CdSe quantum dot doped stabilized micelles. Nano Lett 2:1299–1302.

Dabbousi, B.O., RodriguezViejo, J., Mikulec, F.V., Heine, J.R., Mattoussi, H., Ober, R., Jensen, K.F. and Bawendi, M.G. (1997) (CdSe)ZnS core-shell quantum dots: synthesis and characterization of a size series of highly luminescent nanocrystallites. J Phys Chem B V 101:9463–9475.

de Both, N.J., Vermey, M., Dinjens, W.N. and Bosman, F.T. (1999) A comparative evaluation of various invasion assays testing colon adenocarcinoma cell lines. Br J Cancer 81:934–941.

Dubertret, B., Skourides, P., Norris, D.J., Noireaux, V., Brivanlou, A.H. and Libchaber, A. (2002) *In vivo* imaging of quantum dots encapsulated in phospholipid micelles. Science 298:1759–1762.

Gerion, D., Pinaud, F., Williams, S.C., Parak, W.J., Zanchet, D., Weiss, S. and Alivisatos, A.P. (2001) Synthesis and properties of biocompatible water-soluble silica-coated CdSe/ZnS semiconductor quantum dots. J Phys Chem B 105:8861–8871.

Hines, M.A. and Guyotsionnest, P. (1996) Synthesis and characterization of strongly luminescing ZnS-capped CdSe nanocrystals. J Phys Chem 100:468–461.

Jaiswal, J.K., Mattoussi, H., Mauro, J.M. and Simon, S.M. (2003) Long-term multiple color imaging of live cells using quantum dot bioconjugates. Nat Biotechnol 21:47–51.

Kleinman, H.K., McGarvey, M.L., Hassell, J.R., Star, V.L., Cannon, F.B., Laurie, G.W. and Martin, G.R. (1986) Basement membrane complexes with biological activity. Biochemistry 25:312–318.

Kramer, R.H., Bensch, K.G. and Wong, J. (1986) Invasion of reconstituted basement membrane by metastatic human tumor cells. Cancer Res 46:1980–1989.

Lakka, S.S., Rajagopal, R., Rajan, M.K., Mohan, P.M., Adachi, Y., Dinh, D.H., Olivero, W.C., Gujrati, M., Ali-Osman, F., Roth, J.A., Yung, W.K., Kyritsis, A.P. and Rao, J.S. (2001) Adenovirus-mediated antisense urokinase-type plasminogen activator receptor gene transfer reduces tumor cell invasion and metastasis in non-small cell lung cancer cell lines. Clin Cancer Res 7:1087–1093.

Li, J., Hu, S.X., Perng, G.S., Zhou, Y., Xu, K., Zhang, C., Seigne, J., Benedict, W.F. and Xu, H.J. (1996) Expression of the retinoblastoma (RB) tumor suppressor gene inhibits tumor cell invasion *in vitro*. Oncogene 13:2379–2386.

Moon, A., Kim, M.S., Kim, T.G., Kim, S.H., Kim, H.E., Chen, Y.Q. and Kim, H.R. (2000) H-ras, but not N-ras, induces an invasive phenotype in human breast epithelial cells: a role for MMP-2 in the H-ras-induced invasive phenotype. Int J Cancer 85:176–181.

Murray, C.B., Norris, D.J. and Bawendi, M.G. (1993) Synthesis and characterization of nearly monodisperse CdE (E = S, Se, Te) semiconductor nanocrystallites. J Am Chem Soc 115:8706–8715.

Nawrocki Raby, B., Polette, M., Gilles, C., Clavel, C., Strumane, K., Matos, M., Zahm, J.M., Van Roy, F., Bonnet, N. and Birembaut, P. (2001) Quantitative cell dispersion analysis: new test to measure tumor cell aggressiveness. Int J Cancer 93:644–652.

Noel, A.C., Calle, A., Emonard, H.P., Nusgens, B.V., Simar, L., Foidart, J., Lapiere, C.M. and Foidart, J.-M. (1991) Invasion of reconstituted basement membrane matrix is not correlated to the malignant metastatic cell phenotype. Cancer Res 51:405–414.

Parak, W.J., Boudreau, R., Le Gros, M., Gerion, D., Zanchet, D., Micheel, C.M., Williams, S.C., Alivisatos, A.P. and Larabell, C.A. (2002a) Cell motility and metastatic potential studies based on quantum dot imaging of phagokinetic tracks. Adv Mater 14:882–885.

Parak, W.J., Gerion, D., Zanchet, D., Woerz, A., Pellegrino, T., Micheel, C.M., Williams, S., Seitz, M., Bruehel, R., Bryant, Z., Bustamante, C., Bertozzi, C. and Alivisatos, P. (2002b) Conjugation of DNA to silanized colloidal semiconductor nanocrystalline quantum dots. Chem Mater 14:2113–2119.

Ree, A.H., Bjornland, K., Brunner, N., Johansen, H.T., Pedersen, K.B., Aasen, A.O. and Fodstad, O. (1998) Regulation of tissue-degrading factors and *in vitro* invasiveness in progression of breast cancer cells. Clin Exp Metastasis 16:205–215.

Rosenthal, S.J., Tomlinson, I., Adkins, E.M., Schroeter, S., Adams, S., Swafford, L., McBride, J., Wang, Y., DeFelice, L.J. and Blakely, R.D. (2002) Targeting cell surface receptors with ligand-conjugated nanocrystals. J Am Chem Soc 124:4586–4594.

Silvestri, I., Longanesi Cattani, I., Franco, P., Pirozzi, G., Botti, G., Stoppelli, M.P. and Carriero, M.V. (2002) Engaged urokinase receptors enhance tumor breast cell migration and invasion by upregulating α(v)β5 vitronectin receptor cell surface expression. Int J Cancer 102:562–571.

Sliva, D., Mason, R., Xiao, H. and English, D. (2000) Enhancement of the migration of metastatic human breast cancer cells by phosphatidic acid. Biochem Biophys Res Commun 268:471–479.

Terranova, V.P., Hujanen, E.S. and Martin, G.R. (1986) Basement membrane and the invasive activity of metastatic tumor cells. J Natl Cancer Inst 77:311–316.

Wu, M.X., Liu, H., Liu, J., Haley, K.N., Treadway, J.A., Larson, J.P., Ge, N., Peale, F. and Bruchez, M.P. (2003) Immunofluorescent labeling of cancer marker Her2 and other cellular targets with semiconductor quantum dots. Nat Biotechnol 21:41–46.